

Continuous-Variable Quantum Key Distribution with key rates far above the PLOB bound

Arpan Akash Ray¹ and Boris Škorić¹

¹*TU Eindhoven, The Netherlands*

Abstract

Continuous-Variable Quantum Key Distribution (CVQKD) at large distances has such high noise levels that the error-correcting code must have very low rate. In this regime it becomes feasible to implement random-codebook error correction, which is known to perform close to capacity.

We propose a reverse reconciliation scheme for CVQKD in which the first step is advantage distillation based on random-codebook error correction operated above the Shannon limit. Our scheme has a novel way of achieving statistical decoupling between the public reconciliation data and the secret key. We provide an analysis of the secret key rate for the case of Gaussian collective attacks, and we present numerical results. The best performance is obtained when the message size exceeds the mutual information $I(X; Y)$ between Alice's quadratures X and Bob's measurements Y , i.e. the Shannon limit. This somewhat counter-intuitive result is understood from a tradeoff between code rate and frame rejection rate, combined with the fact that error correction for QKD needs to reconcile only random data.

We obtain secret key rates that lie far above the Devetak-Winter value $I(X; Y) - I(E; Y)$, which is the upper bound in the case of one-way error correction. Furthermore, our key rates lie above the PLOB bound for Continuous-Variable detection, but below the PLOB bound for Discrete-Variable detection.

Our scheme opens up the possibility of long-range CVQKD, with key information per photon on par with discrete-variable QKD, and furthermore provides a way to perform error-correction in a massively parallel way, thus allowing for real-time operation.

1 Introduction

1.1 Error correction in Continuous-Variable QKD

Continuous-Variable Quantum Key Distribution (CVQKD) is a variant of QKD that works with weak coherent states and quadrature measurements. It is an attractive QKD variant because of its cost-effectiveness, which is due to the use of standard telecom equipment.

In Discrete-Variable QKD (DVQKD), propagation of light over long distances causes photon loss, which leads to non-detection events at the receiver side. The loss is very easy to deal with: the event is simply discarded. In CVQKD, in contrast, a quadrature observation always results in a measurement outcome. The loss of photons causes a deterioration of the signal-to-noise ratio (SNR) at the receiver's side. The extremely low SNR has to be dealt with by using high-performance error correcting codes. Various codes have been considered for CVQKD. Popular types of code are LDPC codes [1, 2, 3, 4, 5], Turbo codes and Polar codes [6, 7], all of which approach the Shannon limit. (See [8] for an overview.) In QKD it is important not only to be able to correct the errors, but also to do it *in real time*. This is a particularly tough challenge for the decoding step, which is the most computationally demanding. LDPC decoding, for instance, at low rate needs many iterations which cannot be done in parallel.

1.2 Contribution

We propose a reverse reconciliation scheme for long-distance CVQKD, consisting of an advantage distillation step followed by ordinary high-rate error correction. Advantage distillation [9, 10] is a technique that lets Alice and Bob exploit two-way communication to select snippets of raw data for which they have an increased advantage over Eve. Our advantage distillation scheme is essentially random-codebook error correction with a decoder that does a Neyman-Pearson test for each candidate codeword. The decoder *rejects* unless there is exactly one candidate below the decision threshold. The use of random codebooks is motivated by two observations: (i) random codebooks get close to the Shannon limit; (ii) at the very low rates dictated by long-distance CVQKD, the number of codewords is limited and it becomes feasible to actually implement a random codebook.

We provide a security analysis for the case of Gaussian collective attacks, looking at asymptotics only, i.e. without finite size effects. It has been shown [11, 12] that Gaussian attacks are optimal against a variety of CVQKD schemes, though not necessarily schemes that do postselection. (See Section 6 for a discussion of this point.)

In information reconciliation it is advantageous to work with ‘decoupled’ error correction data, i.e. redundancy data that is statistically independent from the secret. We achieve decoupling by first mapping Bob’s measurements, which are Gaussian-distributed, to uniform variables on the interval $(0, 1)$ and then adding these values (modulo 1) to the random codeword entries which are also uniform on $(0, 1)$. In Discrete Variable QKD the equivalent would be to XOR a binary codeword into a binarisation of Y . Our decoupling technique is more versatile than the octonion-based approach of Leverrier et al [13], and avoids their ‘no go theorem’ that allows only 8-dimensional subspaces. Furthermore, our processing of Y retains distance information that is lost in common techniques like bit slicing [14] and Gray coding.

We present a theoretical analysis of our scheme as well as numerical results, working with Gaussian modulation for simplicity. We focus on small values of the transmission parameter T . The main figure of merit is the **secret key ratio** (SKR), the number of derived key bits per coherent state sent. Having the option of accepting/rejecting yields an expression for the achievable SKR of the form

$$P_{\text{acc}}^{\text{av}} \left[\gamma \cdot (1 - h(\text{BER}^{\text{av}})) \cdot I(X_i; Y_i) - I(E_i; Y_i) \right]. \quad (1)$$

Here $P_{\text{acc}}^{\text{av}}$ is the average accept probability, X_i is Alice’s i ’th quadrature value, Y_i is Bob’s corresponding quadrature, E_i is Eve’s quantum system, I stands for mutual information, h is the binary entropy function, BER^{av} is the average bit error rate in the accepted blocks, and γ represents the rate of our error-correcting code relative to the channel capacity $I(X_i; Y_i)$. It turns out that the highest SKR is obtained by setting $\gamma > 1$, even though this causes a high frame reject rate. Having a lot of frame rejections is allowed because QKD does not need the message to be predetermined; Alice and Bob only have to agree on a shared noise-free random string. (Using a code for CVQKD at a rate above capacity is a known option [15].)

We predict SKRs far above the Devetak-Winter value $I(X_i; Y_i) - I(E_i; Y_i)$. The Devetak-Winter rate is an upper bound *for the case of one-way communication*, and hence does not apply in general. Nevertheless, it is often treated as a de facto upper bound, because existing reconciliation schemes have rates below Devetak-Winter and approach it from below as the efficiency of the employed error-correcting code increases. Furthermore, our predicted SKRs lie *above the PLOB bound* [16] for CV-QKD. This is a point that we do not fully understand; see the discussion in Section 6. Other CVQKD schemes that use postselection [17, 18] report secret key ratios below the Devetak-Winter value.

At long distances our SKR is around 10^{-3} key bits per coherent state (see Table 1); the average number of photons in the Gaussian modulation scales as $1/T$. The mechanism underlying our high SKR is that the factor $\gamma[1 - h(\text{BER}^{\text{av}})]$ can be made larger than 1, which is then exploited by increasing the laser power, which widens the (usually very small) gap between $I(X_i; Y_i)$ and $I(E_i; Y_i)$.

Error-correction decoding is the computational bottleneck in CVQKD. Our decoding, based on Neyman-Pearson scores, lends itself to massive parallelisation, which is an enabler to achieve real-time operation.

2 Preliminaries: CVQKD with Gaussian modulation, homodyne detection and reverse reconciliation

We briefly review CVQKD basics. We consider Gaussian modulation, for simplicity. We consider the usual attacker model: Eve can manipulate quantum states in transit, but cannot access Alice and Bob’s laboratories. Alice and Bob communicate over a classical channel that is noiseless, insecure, and authenticated.

Alice draws Gaussian $A_1, A_2 \in \mathbb{R}$ with zero mean and variance σ_X^2 . She sends a coherent state with displacement (A_1, A_2) . Bob randomly measures one of the two quadratures. This procedure is repeated n times. Bob’s outcomes are $Y \in \mathbb{R}^n$. Alice’s displacement components that match Bob’s choice of quadratures are denoted as $X \in \mathbb{R}^n$.

Alice and Bob monitor the noise in the quantum channel. The channel can be characterised by two parameters [19]: the attenuation T and the excess noise power ξ . It holds that $y_i = \sqrt{T}x_i + N_{\text{shot}} + N_{\text{exc}}$ where N_{shot} is shot noise, Gaussian with zero mean and variance $\frac{1}{2}$; the N_{exc} is excess noise, Gaussian with zero mean and variance $T\xi/2$. We do not include the quantum efficiency and electronics noise of the detector in the model, as it can be absorbed in T [20]. The variance of Y_i is

$$\sigma_Y^2 = T\sigma_X^2 + \frac{1}{2} + \frac{1}{2}T\xi \quad \sigma_{Y|X}^2 = \frac{1}{2} + \frac{1}{2}T\xi. \quad (2)$$

In long-distance CVQKD we have $T \ll 1$. In theory it is advantageous to work with high modulation variance, but in practice this causes phase noise [21], which manifests as excess noise. We consider the regime where $T\sigma_X^2 < 1$, $\xi \ll \sigma_X^2$.

Bob informs Alice of his quadrature choices. Bob generates a secret key $K \in \mathcal{K}$, which typically is a hash of some U , where U is an error-correction codeword or a discretisation of Y . He computes information reconciliation data P and sends P to Alice. Typically P contains a seed for the hash and e.g. the syndrome of the discretised Y , or a codeword xor’ed into Y . From X and P Alice reconstructs K by first reconstructing U and then hashing U with the provided seed.

The maximum achievable size of K , in bits, divided by n is called the secret key capacity. It has been shown [22] that the secret key capacity for Gaussian modulation and one-way reverse reconciliation is bounded as

$$C_{\text{secre}}^{\text{Gauss}} \geq I(X_i; Y_i) - I(Y_i; E_i). \quad (3)$$

The mutual information between the classical X_i and Y_i follows from the signal-to-noise ratio,

$$I(X_i; Y_i) = \frac{1}{2} \log_2 \left(1 + \frac{T\sigma_X^2}{\sigma_{Y|X}^2} \right) = T\sigma_X^2 \log_2 e - \mathcal{O}(T^2\sigma_X^4). \quad (4)$$

The leakage $I(Y_i; E_i) = S(E_i) - S(E_i|Y_i)$ is discussed in the Methods.

$$I(E_i; Y_i) = T\sigma_X^2 \log_2 e \cdot \sigma_X^2 \ln \frac{1 + \sigma_X^2}{\sigma_X^2} + \mathcal{O}(T\xi \log \frac{1}{T\xi}) - \mathcal{O}(T^2\sigma_X^4). \quad (5)$$

3 The proposed information reconciliation method

The random-codebook error correction serves as a first step that produces a low-noise binary string, which is then in the second step further corrected using a high-rate code. We do not specify details of the high-rate code, and simply assume that it is able to error-correct at the Shannon bound with arbitrarily low frame rejection rate; This assumption is motivated by the existence of highly efficient codes, such as LDPC codes, which asymptotically achieve capacity.

3.1 Protocol steps

Preparation.

Alice and Bob agree on a number of public parameters: a variance σ_X^2 ; sequence length n ; code size q ; an integer N ; key length L . They agree on a strong extractor function $\text{Ext} : \mathcal{R} \times \{0, 1\}^{N \log_2 q} \rightarrow \{0, 1\}^L$. Furthermore they agree on a binary error-correcting code \mathcal{E} that has codewords of length $N \log_2 q$.

We assume that the channel properties T, ξ are known to Alice and Bob. We write F_Y for the cumulative distribution function of Y , where Y is Gaussian with zero mean and variance σ_Y^2 .

Repeated steps (see Fig. 1):

1. Alice sends n coherent states, using Gaussian modulation. The variance of each quadrature is σ_X^2 . Alice stores the displacements.
2. For each coherent state, Bob randomly chooses a quadrature. The result of the homodyne measurements is denoted as $y \in \mathbb{R}^n$. He generates a random table $w \in [0, 1]^{q \times n}$, where each table entry is uniform and independent. He publishes the table. He picks a random row index $u \in \{1, \dots, q\}$. For all $i \in \{1, \dots, n\}$ he computes

$$\tilde{y}_i = F_Y(y_i) \in (0, 1) \quad \text{and} \quad c_i = \tilde{y}_i + w_{ui} \bmod 1. \quad (6)$$

Bob sends his quadrature choices and $c = (c_1, \dots, c_n)$.

3. Alice constructs a vector $x \in \mathbb{R}^n$ that consists of the transmitted displacements in the direction of Bob's quadrature choices. For each candidate row index $\ell \in \{1, \dots, q\}$ she computes a score $S_\ell(x, w, c)$,

$$S_\ell(x, w, c) = \sum_{i=1}^n \left[F_Y^{\text{inv}}(c_i - w_{\ell i} \bmod 1) - x_i \sqrt{T} \frac{\sigma_Y}{T \sigma_X} \right]^2. \quad (7)$$

She picks a threshold θ which may depend on x . If there exists exactly one index ℓ satisfying $S_\ell < \theta$ then Alice sets $\hat{u} = \ell$ and she **accepts**. In any other case she **rejects**. Alice informs Bob of her **accept/reject** decision.

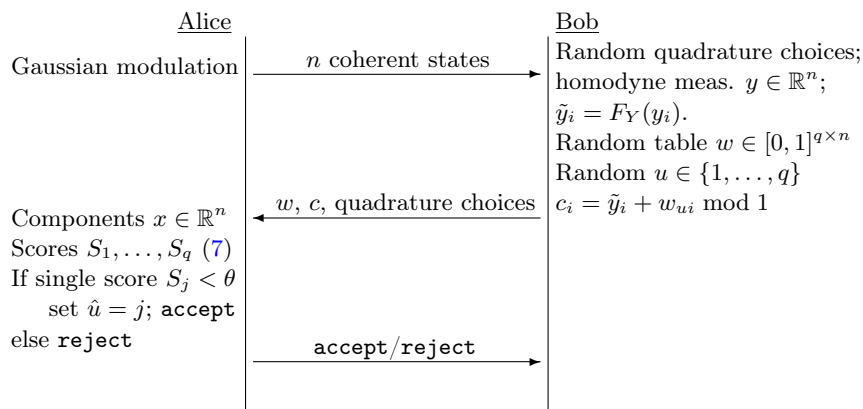


Figure 1: Protocol steps for information reconciliation of one q -ary symbol u .

Finalization.

Alice and Bob collect the indices $u^{(1)}, \dots, u^{(N)}$ from N **accepted** rounds. They convert each of these indices to binary representation and concatenate them; then they use the code \mathcal{E} to get rid of the leftover errors¹ (**accept** events with $\hat{u} \neq u$); finally they perform privacy amplification. The final QKD key is

$$\text{Ext}\left(r, \text{bin } u^{(1)} || \dots || \text{bin } u^{(N)}\right) \in \{0, 1\}^L. \quad (8)$$

Here r is a randomly chosen (public) seed, and ‘bin’ stands for binarisation.

In the Methods we motivate our choice of score function and we explain why the reconciliation data c is statistically independent of u .

¹E.g. Bob sends the one-time-padded syndrome of $\text{bin } u^{(1)} || \dots || \text{bin } u^{(N)}$ to Alice.

4 Analysis

Lemma 4.1. Consider the score system for given x, w, u and random Y . The true-codeword score S_u can be written as $S_u = \sigma_{Y|X}^2 A$, where A follows a noncentral chi-square distribution with parameters (n, λ_1) ,

$$\lambda_1 = n \frac{\sigma_{Y|X}^2}{T\sigma_X^2} \cdot \frac{\frac{1}{n} \sum_i x_i^2}{\sigma_X^2} \approx n \frac{\sigma_{Y|X}^2}{T\sigma_X^2}. \quad (9)$$

The probability that S_u erroneously ends up above the threshold θ is

$$\pi_1(x, w, u) \stackrel{\text{def}}{=} \Pr_Y[S_u > \theta] = Q_{\frac{n}{2}}(\sqrt{\lambda_1}, \sqrt{\theta/\sigma_{Y|X}^2}) \quad (10)$$

where Q is the Marcum Q -function.

Lemma 4.2. Consider the score system for given x, y, u and random W . The wrong-codeword scores S_ℓ ($\ell \neq u$) can be written as $S_\ell = \sigma_Y^2 B_\ell$, where the random variables $(B_\ell)_{\ell \neq u}$ are independent and follow a noncentral chi-square distribution with parameters (n, λ_0) , with

$$\lambda_0 = n \frac{\sigma_Y^2}{T\sigma_X^2} \cdot \frac{\frac{1}{n} \sum_i x_i^2}{\sigma_X^2} \approx n \frac{\sigma_Y^2}{T\sigma_X^2}. \quad (11)$$

The probability that S_ℓ erroneously ends up below θ is

$$\pi_0(x, y, u) \stackrel{\text{def}}{=} \Pr_W[S_\ell < \theta] = 1 - Q_{\frac{n}{2}}(\sqrt{\lambda_0}, \sqrt{\theta/\sigma_Y^2}) \quad \ell \neq u. \quad (12)$$

The proofs are given in the Methods. The lemmas allow us to analytically compute decision error probabilities when the codeword table W is completely uniform. For *pseudorandom* W , Lemma 4.1 still holds, but Lemma 4.2 breaks down; however, for unknown U, Y the argument of $F_Y^{\text{inv}}(\tilde{Y}_i + W_{U_i} - W_{\ell_i} \bmod 1)$ is close to uniform when the table size q is large (ergodicity). Even though the scores S_ℓ ($\ell \neq u$) are not independent for pseudorandom W , the distribution of each S_ℓ viewed individually will closely resemble the distribution specified in Lemma 4.2.

Lemma 4.3. The probability of True Accept (TA) and False Accept (FA) are

$$P_{\text{TA}} = \mathbb{E}_u \Pr[S_u < \theta] \prod_{\ell: \ell \neq u} \Pr[S_\ell > \theta] \quad (13)$$

$$= (1 - \pi_1)(1 - \pi_0)^{q-1} \quad (14)$$

$$P_{\text{FA}} = \mathbb{E}_u \Pr[S_u > \theta] \sum_{a: a \neq u} \Pr[S_a < \theta] \prod_{\ell \notin \{u, a\}} \Pr[S_\ell > \theta] \quad (15)$$

$$= (q-1)\pi_1\pi_0(1 - \pi_0)^{q-2}. \quad (16)$$

Proof: (13) and (15) follow from the decision procedure (Section 3.1). Lines (14), (16) follow by substituting (10,12). \square

We write $P_{\text{acc}} = P_{\text{TA}} + P_{\text{FA}}$. The Symbol Error Rate (SER) σ is defined as the probability that $\hat{u} \neq u$, conditioned on **accept**.

$$\sigma \stackrel{\text{def}}{=} \Pr[S_u > \theta \wedge \exists_{\text{unique } \ell \neq u} S_\ell < \theta \mid \text{accept}] = \frac{P_{\text{FA}}}{P_{\text{TA}} + P_{\text{FA}}} = \frac{(q-1)\pi_0\pi_1}{(1 - \pi_1)(1 - \pi_0) + (q-1)\pi_0\pi_1}. \quad (17)$$

Secret key ratio.

We introduce a parameter γ as the rate of the random code divided by the channel capacity,

$$\log_2 q = \gamma I(X; Y). \quad (18)$$

Furthermore we introduce an x -dependent threshold choice for Alice,

$$\theta = \sigma_{Y|X}^2 \lambda_1 + n\alpha \quad (19)$$

where α is a parameter. The x -dependence enters only via the combination $m \stackrel{\text{def}}{=} \sigma_X^{-2} \sum_i x_i^2$. We use (γ, α) as designer degrees of freedom instead of (n, θ) .

Alice and Bob concatenate N blocks of $\log_2 q$ bits; these blocks have different m -dependent SER σ . The overall SER in the concatenated string is $\sigma^{\text{av}} \approx \mathbb{E}_m \sigma$. Assuming a good code \mathcal{E} that performs close to the Shannon limit, the error correction leads to a factor $1 - h(\text{BER})$ in the amount of secret data, where BER is the Bit Error Rate that \mathcal{E} can handle. The SER σ^{av} leads to $\text{BER} = \sigma^{\text{av}}/2$; a symbol error results in a random index $\hat{u} \neq u$, whose binary representation contains 50% bit flips with respect to u .

The size of the built up raw secret is proportional to the frame accept probability P_{acc} . The P_{acc} depends on m . We define $P_{\text{acc}}^{\text{av}} = \mathbb{E}_m P_{\text{acc}}$. On average the key length is $L = P_{\text{acc}}^{\text{av}} \cdot N \log q \cdot [1 - h(\frac{\sigma^{\text{av}}}{2})] - P_{\text{acc}}^{\text{av}} \cdot N \cdot nI(E_i; Y_i)$. The SKR is $R = \frac{L}{Nn}$. With $\log q = \gamma nI(X_i; Y_i)$, we get

$$R = P_{\text{acc}}^{\text{av}} \left[\gamma \left[1 - h\left(\frac{\sigma^{\text{av}}}{2}\right) \right] I(X_i; Y_i) - I(E_i; Y_i) \right] \quad (20)$$

$$\stackrel{(4,5)}{=} P_{\text{acc}}^{\text{av}} T \log(e) \cdot \sigma_X^2 \left[\gamma \left[1 - h\left(\frac{\sigma^{\text{av}}}{2}\right) \right] - \sigma_X^2 \ln\left(1 + \frac{1}{\sigma_X^2}\right) \right] - \mathcal{O}(T\xi \log \frac{1}{T\xi}) + \mathcal{O}(T^2 \sigma_X^4). \quad (21)$$

5 Numerical results

At a given T , we parameterize the scheme by setting σ_X^2 , q , γ and α . We set the excess noise as $\xi = 0.01 \cdot \sigma_X^2$ because of the prevalence of phase noise [23]. The n follows from (18), $n = \frac{\log_2 q}{\gamma I(X_i; Y_i)}$.

5.1 Secret key ratio ‘landscape’

Fig. 2 captures the most interesting feature of our results. The optimisation procedure produces results with statistical noise. In effect, we predict that $R_{\text{Optimised}}$ hardly varies with T . As a result, our protocol outperforms the CV PLOB at long distances. Fig. 3a shows how the SKR (20) behaves as a function of the parameters α and γ at $T = 0.001$. At smaller T the picture is very similar (Fig. 3b). There is a long diagonal slope in the (α, γ) -plane, to the ‘northeast’ of the maximum, where the SKR plummets below zero. Note that the SKR is negative at $\gamma < 1$. This is caused by the large modulation variance, which gives rise to a factor $\approx \beta - 1$ in (35). Fig. 4ab shows cross sections through the contour plot.

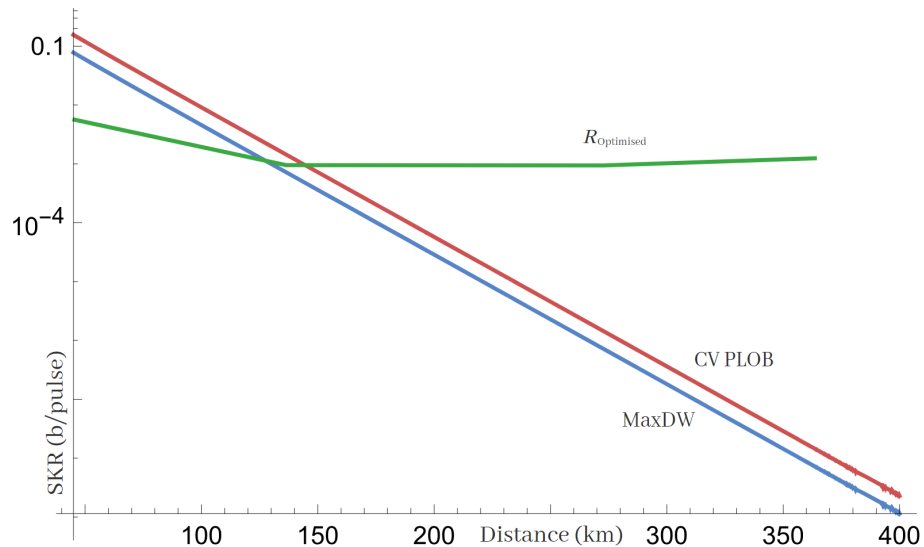
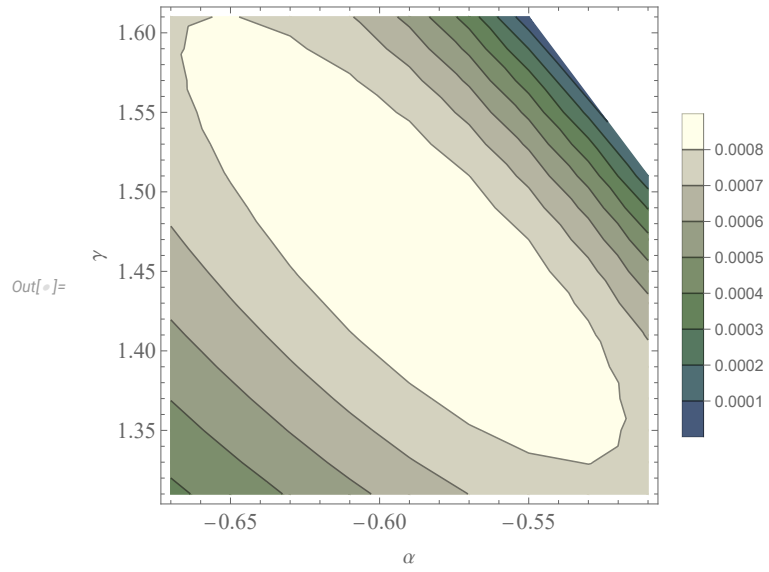
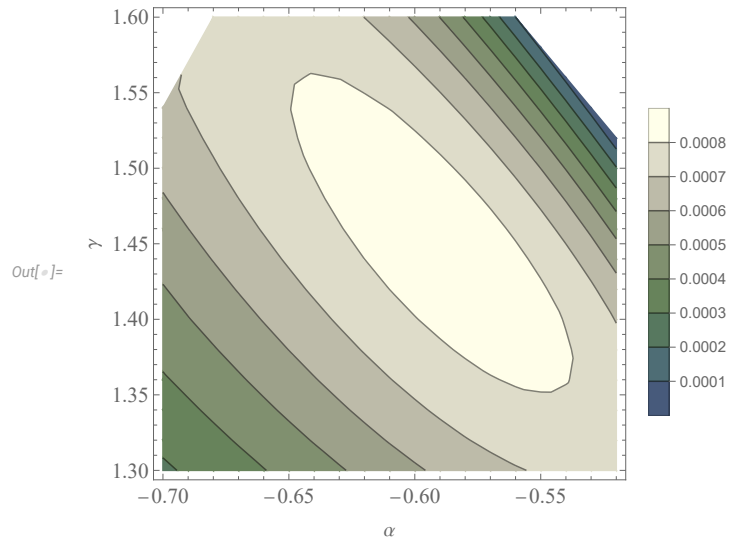


Figure 2: $R_{\text{Optimised}}$, the secret key rate of our protocol with optimised parameters (γ , α and modulation variance σ_x^2) compared to the CV PLOB and MaxDW. MaxDW stands for the maximally achievable Devetak-Winter value at $\xi \rightarrow 0$ and depends only on T . We assume optical fiber with loss of 0.22 dB/km.

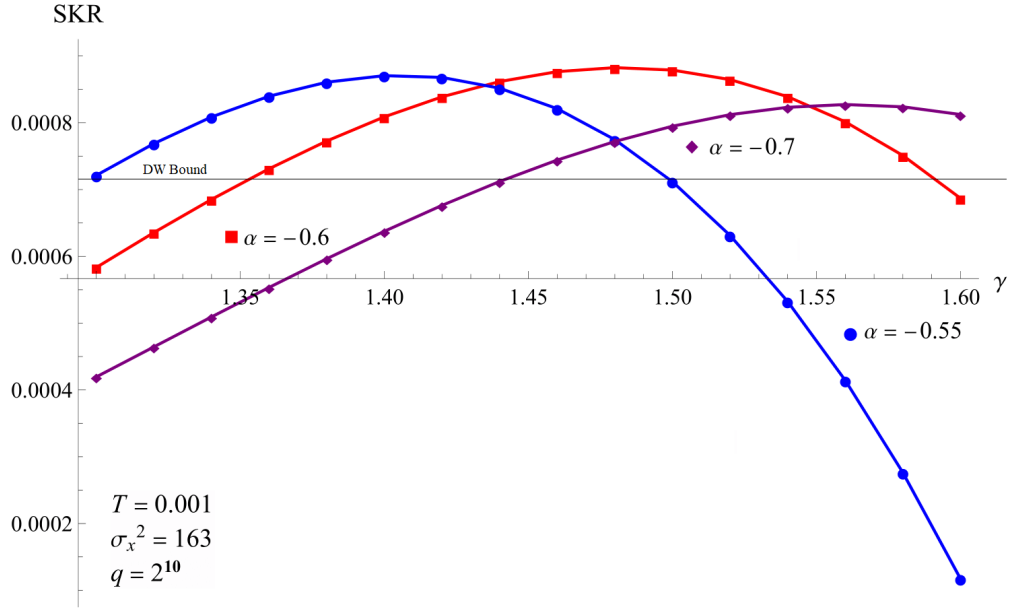


(a) $T = 10^{-3}$, $\sigma_X^2 = 163$

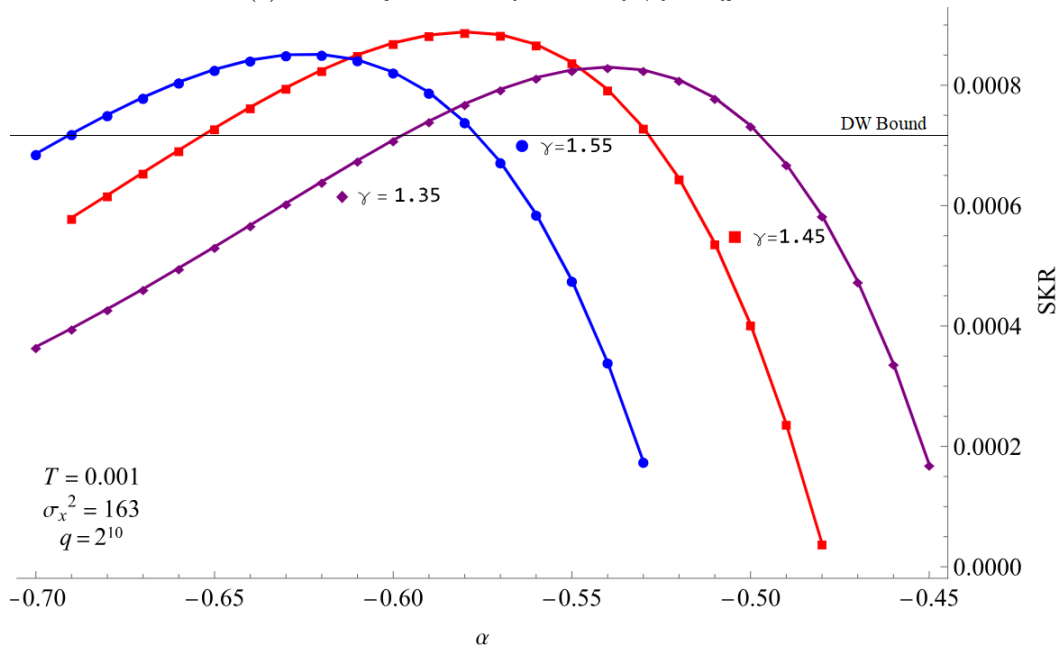


(b) $T = 10^{-6}$, $\sigma_X^2 = 1.7 \times 10^5$

Figure 3: Contour plot of the Secret Key Ratio as a function of α and γ , for $q = 2^{10}$. Negative SKR is shown as white.



(a) Secret key ratio as a function of γ for different α .



(b) Secret key ratio as a function of α for different γ .

Figure 4: Secret key ratio as a function of α and γ , for fixed T, σ_x^2, q and for non zero excess noise (ξ). The DW bound is the maximally achievable Devetak-Winter value at $\xi \rightarrow 0$.

5.2 Secret Key Ratio with unrestricted modulation variance

Table 1 shows high-performance SKR results for several combinations (T, q) . At given (T, q) we tweaked $\alpha, \gamma, \sigma_X^2$ to obtain high SKR; the $n, P_{TA}, P_{FA}, SER, SKR$ follow. We observe that α, γ need to be varied only weakly when the distance is increased. Furthermore the modulation variance σ_X^2 scales as $1/T$. The obtained SKR values hardly vary as a function of T .

Table 1: Optimised scheme parameters for various values of T and q , without restriction on the modulation variance and for non zero ξ . The $maxDW$ stands for the maximally achievable Devetak-Winter value at $\xi \rightarrow 0$ and depends only on T . The relation between T and distance assumes a loss of 0.22 dB/km.

T (Distance) $MaxDW$ $PLoB$	q	α	γ	σ_X^2	n	P_{TA}	P_{FA}	SER	SKR
10^{-1} (45 km) $7.2 \cdot 10^{-2}$ $1.4 \cdot 10^{-1}$	2^5	-0.25	1.15	0.5	64	0.288	0.0286	0.100	0.00486
	2^8	-0.25	1.1	0.8	68	0.222	0.0124	0.058	0.00555
	2^{10}	-0.25	1.15	0.9	77	0.197	0.0115	0.059	0.00576
	2^{20}	-0.25	1.30	1.2	99	0.066	0.0109	0.081	0.00294
10^{-3} (136 km) $7.2 \cdot 10^{-4}$ $1.4 \cdot 10^{-3}$	2^5	-0.90	1.80	77	27	0.035	0.0029	0.108	0.00077
	2^8	-0.65	1.55	101	39	0.037	0.0017	0.065	0.00091
	2^{10}	-0.55	1.45	134	41	0.038	0.0013	0.049	0.00095
	2^{20}	-0.40	1.70	195	65	0.027	0.0003	0.020	0.00094
10^{-6} (273 km) $7.2 \cdot 10^{-7}$ $1.4 \cdot 10^{-6}$	2^5	-0.95	1.90	$8.44 \cdot 10^4$	24	0.029	0.0024	0.113	0.00074
	2^8	-0.65	1.55	$9.62 \cdot 10^4$	41	0.037	0.0016	0.060	0.00088
	2^{10}	-0.55	1.45	$1.20 \cdot 10^5$	45	0.039	0.0013	0.047	0.00094
	2^{20}	-0.40	1.30	$1.88 \cdot 10^5$	67	0.027	0.0003	0.020	0.00092
10^{-8} (364 km) $7.2 \cdot 10^{-9}$ $1.4 \cdot 10^{-8}$	2^5	-0.85	1.75	$8.88 \cdot 10^6$	25	0.039	0.0029	0.102	0.00093
	2^8	-0.60	1.50	$1.10 \cdot 10^7$	38	0.045	0.0021	0.062	0.00114
	2^{10}	-0.50	1.40	$1.18 \cdot 10^7$	49	0.053	0.0019	0.067	0.00124
	2^{20}	-0.35	1.25	$1.90 \cdot 10^7$	69	0.044	0.0008	0.024	0.00136

6 Discussion

The idea of random codebooks is simple, but it is impractical to implement under normal circumstances. In long-distance CVQKD, however, it becomes feasible to implement random codebooks, because of the extremely low code rates. We have investigated this idea, making three design choices: (i) analog xor-ing of \tilde{y} and a random codeword; (ii) Neyman-Pearson testing per candidate codeword; (iii) thresholding with acceptance only if there is a single candidate below θ . The analog xor achieves statistical decoupling of C and U without needing 8-component parts of Y . The thresholding introduces a frame rejection mechanism, allowing us to work with efficiency $\gamma > 1$. In the Methods we comment on implementation aspects.

Collective attacks and general attacks.

The presented key rate analysis is for the case of Gaussian collective attacks. However, the results hold more generally for arbitrary collective attacks. (i) In the asymptotic regime it is known that Gaussian attacks are optimal among all the collective attacks [24, 25, 12].

(ii) Alice and Bob can apply channel monitoring: instead of just estimating the first and second moment of the empirical distribution, they determine if the empirical distribution of Y given X looks sufficiently Gaussian, and reject if it does not [26]. In the case of collective attacks this monitoring procedure can be effectively implemented, since typically one works with block sizes of 10^7 to 10^8 samples. In our scheme it helps that all states associated with *rejects*, i.e. the majority,

become available for channel monitoring.

The de Finetti theorem [27, 28] and ‘Postselection’ technique [29] lift security against collective attacks to security against general attacks, in the asymptotic limit. The more efficient version of this ‘upgrade’ [27], with manageable finite-size penalties, typically does not apply for CVQKD schemes that have postselection. It is an open problem to determine whether our scheme is compatible with the symmetrisation operations in [27]. Our postselection differs from other schemes in the literature by selecting low-shotnoise sequences, with very weak dependence on X , as opposed to the more usual rejection of predetermined Y -regions in phase space. In particular, the most important selection criteria (the random codewords) *do not yet exist* at the moment when Eve has to attack the quantum states. Intuitively, one would expect that this nonexistence implies that Eve cannot devise any advantageous way to manipulate the postselection procedure, i.e. cannot find a better attack than the Gaussian attack.

The PLOB bound.

We find that we predict secret keys rates above the PLOB bound for CV-QKD, which is $-\log(1 - T) = \frac{T}{\ln 2} + \mathcal{O}(T^2)$ bits per channel use, where sending a coherent state counts as one channel use. (But we are well below the PLOB bound for DV-QKD.) Naturally this raises the question if something is wrong with our security analysis or with the PLOB bound. We believe that our key rates are correct at least in the asymptotic case.

The PLOB bound on the CV-QKD rate has a peculiarity: the CV key rate *per sent photon* is lower by a factor $\approx T$ than the bound for DV. Intuitively this can be understood from the fact that in CV Eve obtains a fraction $1 - T$ of the sent quadrature information, and Bob a only fraction T . In order to obtain a signal-to-noise ratio of $\mathcal{O}(1)$ at Bob’s lab, and thus achieve $\mathcal{O}(1)$ bits of non-secret information, Alice has to send $\mathcal{O}(1/T)$ photons in a coherent state. Sending one coherent state counts as one channel use. The corresponding amount of secret information per channel use is $\mathcal{O}(T)$; counted per sent photon that yields $\mathcal{O}(T^2)$.

This scaling is also visible in the mutual information expressions at $T \ll 1$. In the reverse reconciliation, Alice and Eve have nearly identical information from which they have to reconstruct Bob’s value Y . From the equations at $T \ll 1$ (3,4), setting $\sigma_X^2 = \mathcal{O}(1/T)$, we see that both Alice and Eve obtain mutual information $\mathcal{O}(1)$ per coherent state, and that the difference between Alice and Eve is $\mathcal{O}(T)$. *Crucially, our advantage distillation widens this gap to $\mathcal{O}(1)$.* It does this by selecting sequences that contain low average shot noise, thus artificially improving the signal-to-noise ratio by postprocessing.

In DV the situation is entirely different. Here post-selection occurs naturally, namely by single-photon detection, and the selected events have very little leakage. A fraction T of photons survive the voyage. Of any photon that survives, the secret information is $\mathcal{O}(1)$ (the details depend on the bit error rate on the quantum channel). This results in $\mathcal{O}(T)$ secret information per sent photon.

A quadrature measurement may be used as a low-quality single-photon detection, in such a way that the quality of the detection does not depend on T . This blurs the distinction between DV and CV measurements, and raises the question why there should be an $\mathcal{O}(T)$ difference in the secret key capacity per sent photon for CV versus DV. Our results seem to indicate that a CV measurement plus postprocessing can become similar to a DV measurement. We mention that the gaussianity-preserving postselection scheme of [11] is mathematically equivalent to a noiseless amplification of the quantum signal. In that scheme quadratures far away from the origin are favored, which actually allows Bob to better distinguish between vacuum and non-vacuum.

Remark: Key rates above the CV PLOB bound have also been reported [30] in a more simple scheme than ours. There the advantage distillation is done with a short linear code operated above capacity.

Future work.

We mention the following topics for future work.

- The compatibility of our scheme with state symmetrisations.
- For the variables \tilde{y}_i and the codebook entries w_{ℓ_i} we have assumed a fine-grained discretisation of the interval $[0, 1]$, essentially a continuum. It needs to be determined how coarse the discretisation can be made.

- Our analysis assumes independent random codebook entries. Pseudorandomness may suffice, depending on the seed entropy.
- Alternative decision procedures may be considered, e.g. rejecting only when all scores lie above θ .
- The threshold θ may be set in a different way.
- Alice may use the value m as soft information for the error correction. Ideally that would yield a SKR that is the m -average of (1).
- In the protocol as specified in Section 3.1, a new table w is generated for each q -ary symbol that Bob tries to send to Alice. We have chosen for this approach in order to make sure that Eve does not possess any symmetry-breaking information at the moment when she has to attack the quantum states. It may well be that it is also safe to re-use a table for multiple symbols.

Acknowledgements

We gratefully acknowledge discussions with João dos Reis Frazão, Kadir Gümüüş, and Basheer Joudeh. Part of this work was supported by the Dutch Groeifonds QDNL KAT-2 and by the Forwardt project (NWO CS.001).

7 Methods

7.1 Notation and terminology

Stochastic variables are written in capital letters, and their numerical values in lowercase. The notation $\Pr[X = x]$ stands for the probability that the random variable X takes value x . The expectation over X is defined as $\mathbb{E}_x f(x) = \sum_x \Pr[X = x]f(x)$. The Shannon entropy of a random variable X is denoted as $H(X)$. We write h for the binary entropy function, $h(p) = p \log_2 \frac{1}{p} + (1-p) \log_2 \frac{1}{1-p}$. ‘ln’ is the natural logarithm. We measure all entropies in bits. The mutual information between X and Y is written as $I(X; Y)$. The entropy of Y given X is written as $H(Y|X) = \mathbb{E}_x H(Y|X = x)$. A quantum state is described by a density matrix ρ . We write $S(\rho) = -\text{tr} \rho \log_2 \rho$ for the von Neumann entropy of ρ . Consider a joint classical-quantum state of a classical random variable Y and a quantum system E that is correlated with Y . The von Neumann entropy of the quantum system given Y is denoted as $S(E|Y) = \mathbb{E}_y S(E|Y = y)$. The mutual information between E and Y is $I(E; Y) = S(E) - S(E|Y)$. In CVQKD the following function often occurs in the calculation of entropies,

$$g(x) \stackrel{\text{def}}{=} (x+1) \log_2(x+1) - x \log_2 x. \quad (22)$$

As the figure of merit of a CVQKD scheme we use the Secret Key **Ratio** (SKR), which equals the length of the constructed secret key divided by the number of laser pulses. This is different from the key *rate* (key bits per second). With the key *ratio* it is possible to do a fair comparison between post-processing schemes of CVQKD setups that have a different number of pulses per second. Note that we do not take into account any pulses that are used solely for channel monitoring.

7.2 Useful lemmas

Lemma 7.1. *Let X_1, \dots, X_n be Gaussian random variables with mean μ_i and unit variance. The distribution of the variable $Z = \sum_{i=1}^n X_i^2$ is the noncentral chi-square distribution with n degrees of freedom and noncentrality parameter $\lambda = \sum_{i=1}^n \mu_i^2$. The expected value of Z is $n + \lambda$, and the variance is $2n + 4\lambda$. The cumulative distribution of Z is given by $F_Z(z) = 1 - Q_{\frac{n}{2}}(\sqrt{\lambda}, \sqrt{z})$, where Q is the Marcum Q -function.*

Lemma 7.2 (Neyman-Pearson). *Let $X \in \mathcal{X}$ be a random variable distributed according to $X \sim P_\theta$, where either $\theta = 0$ or $\theta = 1$. A hypothesis test function is a function $f : \mathcal{X} \rightarrow \{0, 1\}$ that tries to determine the parameter θ from the observed data x . Let $\mathbb{E}_{X \sim P_0} f(X)$ be the type I error probability*

of the test function, and $\mathbb{E}_{X \sim P_1}[1 - f(X)]$ the type II error probability. The likelihood ratio test with threshold k is given by

$$\varphi_k(x) = \begin{cases} 1 & : \frac{P_1(x)}{P_0(x)} > k \\ 0 & : \frac{P_1(x)}{P_0(x)} < k \end{cases}. \quad (23)$$

At a fixed type I error probability, the likelihood ratio test (23) has the lowest type II error probability of all test functions.

Lemma 7.3. *A test function obtained by applying a monotone function to the likelihood ratio $\frac{P_1(x)}{P_0(x)}$ and to the threshold is equivalent to the likelihood ratio test.*

7.3 The leakage

The mutual information $I(E_i; Y_i)$ follows from the symplectic eigenvalues ν_1, ν_2 of Eve's pre-measurement state ρ^{E_i} and the symplectic eigenvalue ν_3 of the (homodyne) post-measurement state $\rho_{y_i}^{A_i}$ [19].

$$I(Y_i; E_i) = g\left(\frac{\nu_1 - 1}{2}\right) + g\left(\frac{\nu_2 - 1}{2}\right) - g\left(\frac{\nu_3 - 1}{2}\right), \quad (24)$$

with g the thermal entropy function as defined in Section 7.1 and

$$\nu_{1,2}^2 = \frac{\Delta \pm \sqrt{\Delta^2 - 4D}}{2} \quad \nu_3^2 = V \left[V - \frac{T(V^2 - 1)}{2\sigma_Y^2} \right] \quad (25)$$

$$\Delta \stackrel{\text{def}}{=} V^2 + [2\sigma_Y^2]^2 - 2T(V^2 - 1) \quad D \stackrel{\text{def}}{=} \left[V \cdot 2\sigma_Y^2 - T(V^2 - 1) \right]^2 \quad (26)$$

where $V = 1 + 2\sigma_X^2$.

7.4 Decoupled reconciliation data

The SKR of CVQKD in practice is affected by the efficiency β of the employed error-correction code ($\beta < 1$) and by the leakage caused by the public reconciliation data P . Furthermore the error-correction code has a failure probability P_{fail} , which limits the key size. A high SKR is obtained by using a highly efficient error-correcting code and leakage-free reconciliation data. Good codes for CVQKD achieve $\beta \approx 0.95$ to 0.98 . Leakage-free reconciliation data is achieved either by sending a one-time-pad-encrypted syndrome or by the trick described below.

Lemma 7.4 (Lemma 1 in [13]). *Let U and P be independent classical random variables. Let E be a quantum system. Then $I(U; PE) \leq I(UP; E)$.*

Corollary 7.5 (Adapted from [13] to the case of reverse reconciliation). *Let X and Y be the measurement result of Alice and Bob respectively. Let E be Eve's quantum system. Let U be a secret chosen by Bob, independent of Y . Let P be public information reconciliation data computed from Y and U , such that Alice is able to reconstruct U from P and X . Let P be statistically independent from U . Then*

$$I(U; PE) \leq I(Y; E). \quad (27)$$

Proof: Lemma 7.4 gives $I(U; PE) \leq I(UP; E)$. Since P is computed from U and Y , it holds that $H(UP) \leq H(UY)$ and $I(UP; E) \leq I(UY; E)$. Finally, we use that Bob chooses the U independently of Y , which allows us to write $I(UY; E) = I(Y; E)$. \square

For the SKR in case of collective attacks this yields

$$R_{\text{key}}^{(\text{decoupled})} \geq (1 - P_{\text{fail}}) \left\{ \beta I(X_i; Y_i) - I(Y_i; E_i) \right\}. \quad (28)$$

In [13] the decoupling of C from U is achieved by taking 8-dimensional subspaces and using the algebraic properties of octonions.

7.5 Statistical decoupling in our scheme

The decoupling between the information reconciliation data (w, c) and the codeword index u , required for the use of Corollary 7.5, is ensured by the uniformity of Y_i , combined with the modulo-1 addition. Adding the uniform variable \tilde{Y}_i to w_{ui} modulo 1 is the analog version of a one-time-pad xor mask, and completely hides w_{ui} .

Lemma 7.6. *Let C be constructed as $c_i = \tilde{y}_i + w_{ui} \bmod 1$. Let $P = (W, C)$. Then the variables P and U are independent.*

Proof: $f_{U|WC}(u|wc) = \frac{f_{UWC}(uwc)}{f_{WC}(wc)} = \frac{f_U(u)f_W(w)f_{C|UW}(c|uw)}{f_W(w)\mathbb{E}_{u'}f_{C|UW}(c|u'w)} = f_U(u) \frac{\prod_i f_{\tilde{Y}}(c_i - w_{ui} \bmod 1)}{\mathbb{E}_{u'} \prod_i f_{\tilde{Y}}(c_i - w_{u'i} \bmod 1)}$
 $= f_U(u) \frac{1}{\mathbb{E}_{u'} 1} = f_U(u)$. Here we have used that \tilde{Y}_i is uniform on $[0, 1]$. \square

Note that our mechanism for achieving independence between C and U is more versatile than the trick introduced by [13], which acts only on 8 components of Y at a time. Our procedure works with any sequence length n as a whole. Furthermore, [13] mentions that decoupling cannot be achieved in dimension higher than $d = 8$, because of the requirement that there must exist exactly $d - 1$ independent vector fields on the unit sphere in \mathbb{R}^d . However, that line of reasoning applies only because they entirely discard the radial degree of freedom in \mathbb{R}^d . By *not* discarding the information contained in $|Y|$, we give ourselves the freedom to introduce decoupling as in (6) simply via the uniform \tilde{y}_i .

7.6 Motivation of the score function (7)

Alice is faced with a one-out-of- q decision problem. This type of problem does not have a known optimal solution. Instead we resort to an often used alternative: to run q binary decision problems. For each candidate row index $\ell \in \{1, \dots, q\}$ Alice tests the binary hypothesis “does u equal ℓ ?” given the data (x, w, c) available to her. For the *binary* hypothesis test we know that the optimal solution is to use the Neyman-Pearson score (23), i.e. the likelihood ratio, or a monotone function of it. The q individual scores can then somehow be combined to obtain a one-out-of- q decision. One example would be to decide on the index ℓ with the highest Neyman-Pearson score; this is similar to a Maximum A Posteriori (MAP) approach. Instead we work with a threshold that is applied to each individual Neyman-Pearson score. Our motivation for this choice is that it lends itself to analysis, and allows for a reject mechanism.

Below we show that the score (7) is equivalent to the Neyman-Pearson score.

Lemma 7.7. *Consider the hypothesis testing problem of Lemma 7.2. Using the expression $\Pr[\theta = 1|X = x]$ as a score function is equivalent to using the likelihood ratio as a score function.*

Proof:

$$\begin{aligned} \frac{P_1(x)}{P_0(x)} &= \frac{\Pr[X = x|\theta = 1]}{\Pr[X = x|\theta = 0]} = \frac{\Pr[X = x]\Pr[\theta = 1|X = x]/\Pr[\theta = 1]}{\Pr[X = x]\Pr[\theta = 0|X = x]/\Pr[\theta = 0]} = \frac{\Pr[\theta = 0]}{\Pr[\theta = 1]} \cdot \frac{\Pr[\theta = 1|X = x]}{\Pr[\theta = 0|X = x]} \\ &= \frac{\Pr[\theta = 0]}{\Pr[\theta = 1]} \cdot \frac{\Pr[\theta = 1|X = x]}{1 - \Pr[\theta = 1|X = x]}. \end{aligned} \quad (29)$$

It follows that $\Pr[\theta = 1|X = x] = \psi\left(\frac{P_1(x)}{P_0(x)}\right)$, with $\psi(z) = \left(1 + \frac{1}{z} \cdot \frac{\Pr[\theta=0]}{\Pr[\theta=1]}\right)^{-1}$. We use that ψ is a monotone increasing function and invoke Lemma 7.3. \square

Lemma 7.8. $\Pr[U = \ell|xwc] \propto \exp\left[-\frac{T\sigma_X^2}{2\sigma_Y^2\sigma_{Y|X}^2} S_\ell(x, w, c)\right]$, with S_ℓ as defined in (7).

Proof:

$$\Pr[U = \ell | xwc] = \frac{\Pr[U = \ell] f_W(w) f_X(x) f_{C|UWX}(c|\ell wx)}{f_W(w) f_X(x) f_{C|WX}(c|wx)} = \frac{1}{q} \cdot \frac{f_{C|UWX}(c|\ell wx)}{f_{C|WX}(c|wx)} \quad (30)$$

$$\propto f_{C|UWX}(c|\ell wx) = \prod_{i=1}^n f_{\tilde{Y}|X}(c_i - w_{\ell i} \bmod 1 | x_i) \quad (31)$$

$$\stackrel{(a)}{\propto} \prod_i \frac{f_{Y|X}(F_Y^{\text{inv}}(c_i - w_{\ell i} \bmod 1) | x_i)}{f_Y(F_Y^{\text{inv}}(c_i - w_{\ell i} \bmod 1))} \quad (32)$$

$$\propto \prod_i \exp - \left(\frac{[F_Y^{\text{inv}}(c_i - w_{\ell i} \bmod 1) - x_i \sqrt{T}]^2}{2\sigma_{Y|X}^2} - \frac{[F_Y^{\text{inv}}(c_i - w_{\ell i} \bmod 1)]^2}{2\sigma_Y^2} \right) \quad (33)$$

$$\propto \prod_i \exp - \frac{\sigma_Y^2 - \sigma_{Y|X}^2}{2\sigma_Y^2 \sigma_{Y|X}^2} \left[F_Y^{\text{inv}}(c_i - w_{\ell i} \bmod 1) - x_i \sqrt{T} \frac{\sigma_Y^2}{\sigma_Y^2 - \sigma_{Y|X}^2} \right]^2. \quad (34)$$

In (a) we used that for a monotone function φ the pdf of $Z = \varphi(Y)$ is given by $f_{Z|X}(z|x) = f_{Y|X}(y|x)/\varphi'(y) = \frac{f_{Y|X}(\varphi^{\text{inv}}(z)|x)}{\varphi'(\varphi^{\text{inv}}(z))}$. Then the special choice $\varphi = F_Y$ yields $f_{Z|X}(z|x) = \frac{f_{Y|X}(F_Y^{\text{inv}}(z)|x)}{f_Y(F_Y^{\text{inv}}(z))}$. Finally, the z in this expression equals \tilde{y}_i given $u = \ell$, w and c , which evaluates to $\tilde{y}_i = c_i - w_{\ell i} \bmod 1$. \square

Finally, since $\exp[-\text{const} \cdot S_\ell]$ is a monotone function of S_ℓ , our score function (7) is equivalent to the Neyman-Pearson score. Due to the minus sign, a *low* score indicates a high likelihood that that the hypothesis is true.

7.7 Thresholding; error types

Alice's decision procedure leads to a number of cases that can occur, listed in Table 2.

Case	Scores	Decision	Comment
1	$S_u < \theta, \forall_{\ell \neq u} S_\ell > \theta$	accept	True Accept
2	$S_u > \theta, \exists_{\text{unique } \ell} S_\ell < \theta$	accept	False Accept
3	$S_u > \theta; S_\ell < \theta$ for several ℓ	reject	justified reject
4	$\forall_\ell S_\ell > \theta$	reject	S_u might be smallest score
5	$S_u < \theta, \exists_{\ell \neq u} S_\ell < \theta$	reject	S_u might be smallest score

Table 2: Possible score configurations leading to Alice's **accept/reject** decision.

An alternative procedure could be to always accept the row index with the lowest score, without ever **rejecting**. In cases 4 and 5 that would be likely to extract correct information, whereas our scheme discards the data. However, case 3 would certainly produce a symbol error, and case 4 and 5 would potentially cause a symbol error. Furthermore, excluding the option of **rejecting** would cause massive symbol error rates when operating above capacity.

Another alternative could be to **reject** only when all scores are above θ . When there are multiple scores *below* θ , there is still a good chance that S_u is the lowest. Analysis of different decision procedures is left for future work.

7.8 Proof of lemmas

Lemma 4.1 At $\ell \neq u$ the expression $C_i - W_{\ell i} \bmod 1$ evaluates to $\tilde{y}_i + W_{ui} - W_{\ell i} \bmod 1$. Since all the $W_{\ell i}$ are independent and uniform, we find that $F_Y^{\text{inv}}(\tilde{y}_i + W_{ui} - W_{\ell i} \bmod 1)$ is an independent Gaussian variable with zero mean and variance σ_Y^2 . Crucially, it is independent of x . We can write $S_\ell = \sum_{i=1}^n [\sigma_Y M_{\ell i} - x_i \sqrt{T} \frac{\sigma_Y^2}{T\sigma_X^2}]^2$, where the $M_{\ell i}$ are independent and normal-distributed. Written as $S_\ell = \sigma_Y^2 \sum_{i=1}^n [M_{\ell i} - x_i \sqrt{T} \frac{\sigma_Y}{T\sigma_X^2}]^2$ we see that each score equals σ_Y^2 times a noncentral chi-squared variable with n degrees of freedom and noncentrality parameter $\lambda = \sum_i (x_i \sqrt{T} \frac{\sigma_Y}{T\sigma_X^2})^2$. \square

Lemma 4.2 At $\ell = u$ the expression $F_Y^{\text{inv}}(C_i - w_{\ell i} \bmod 1)$ evaluates to $F_Y^{\text{inv}}(\tilde{Y}_i) = Y_i$. This yields $S_u(x, w, C) = \sum_i [Y_i - x_i \sqrt{T} \frac{\sigma_Y}{T \sigma_X^2}]^2$. We write $Y_i = x_i \sqrt{T} + \sigma_{Y|X} N_i$, where the noise N_i is normal-distributed and independent of all other variables. We get $S_u = \sigma_{Y|X}^2 \sum_{i=1}^n [N_i - x_i \sqrt{T} \frac{\sigma_{Y|X}}{T \sigma_X^2}]^2$. This has the form of $\sigma_{Y|X}^2$ times a noncentral χ^2 variable with n degrees of freedom and noncentrality parameter $\lambda = \sum_i (x_i \sqrt{T} \frac{\sigma_{Y|X}}{T \sigma_X^2})^2$. \square

7.9 Secret key ratio at small T , at $\beta < 1$

We consider the SKR expression (28). In the regime $T \sigma_X^2 \ll 1$, $\xi \ll \sigma_X^2$ it holds that

$$\beta I(X_i; Y_i) - I(Y_i; E_i) = \frac{1}{2} T \log_2 e \cdot 2 \sigma_X^2 \left[\beta - \sigma_X^2 \ln \left(1 + \frac{1}{\sigma_X^2} \right) \right] + \dots \quad (35)$$

At given β ($\beta < 1$), the value of σ_X^2 that maximizes this expression scales as $\sigma_X^2 \approx \frac{1}{\sqrt{3} \sqrt{1-\beta}}$. When β is exactly 1, it is in theory advantageous to increase σ_X to infinity. However, the proportionality $1/\sqrt{1-\beta}$ means that the optimal σ_X^2 drops very rapidly; e.g. at $\beta = 0.95$ the optimal σ_X^2 has already dropped to $\mathcal{O}(1)$. Let us define

$$f_\beta(x) = 2x \left[\beta - x \ln \left(1 + \frac{1}{x} \right) \right], \quad (36)$$

so that $\beta I(X_i; Y_i) - I(Y_i; E_i) = \frac{1}{2} T \log_2(e) f_\beta(\sigma_X^2)$. Note that $\lim_{x \rightarrow \infty} f_1(x) = 1$. Fig. 5 shows, as a function of β , the value of x that maximizes f_β , as well as the achieved maximum function value.

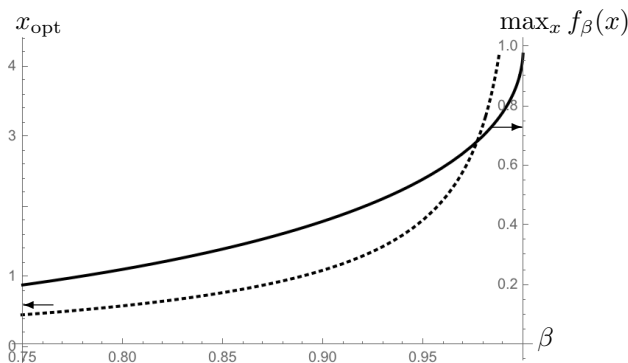


Figure 5: *Solid line:* $\max_x f_\beta(x)$ as a function of β . *Dotted line:* optimal x as a function of β .

7.10 A remark on the secrecy capacity lower bound

Consider a CVQKD scheme that derives the secret key $K \in \{0, 1\}^L$ by hashing a discretisation of Y , and where Bob sends a one-time-padded syndrome to Alice. Asymptotically, use of the Leftover Hash Lemma against quantum adversaries [31] yields that the QKD key is secure if $L < S(Y|E)$. If an accept/reject mechanism exists for blocks of Y , then this condition is modified to $L < P_{\text{acc}} S(Y|E) = P_{\text{acc}} [H(Y) - I(E; Y)]$. The achievable SKR is given by $R = (L - \text{syndrome size})/n$, where the size of the syndrome is subtracted because key material is spent to mask the syndrome. The information reconciliation pertains only to the accepted blocks of Y ; hence the syndrome size also carries a factor P_{acc} . Let us write the syndrome size as $P_{\text{acc}} H(Y|X) \cdot b$. Then² the provably safe SKR is $R < P_{\text{acc}} [H(Y) - bH(Y|X) - I(E; Y)]/n = P_{\text{acc}} [\beta I(X; Y) - I(E; Y)]/n$. Hence (28), with the proper relation between β and P_{acc} inserted, represents a lower bound on the secrecy capacity for any value of β , even $\beta > 1$. Depending on the code, it may happen that (28) achieves a maximum at $\beta > 1$ and that the value exceeds $I(X_i; Y_i) - I(E_i; Y_i)$.

²Typically $b > 1$, meaning that more data is sent than the strictly necessary amount $H(Y|X)$, resulting in $\beta < 1$. A perfect code has $b = 1$ and $\beta = 1$. A code that tries to send a message above the channel capacity has $b < 1$, resulting in $\beta > 1$.

7.11 Implementability

The main implementation hurdle is the sheer size of the codebook w : it has $q \times n$ entries, where q is exponential in the message length. One could consider storing the whole codebook in a memory. The drawback is (a) huge memory requirements; (b) long access times fetching table entries. A more practical approach is to pseudorandomly generate codebook entries on the fly without accessing RAM. PRNG algorithms have been reported that generate 64 to 128 bits of pseudorandomness per nanosecond per core [32, 33]. Let b denote the baud rate, i.e. the number of pulses per second. In the time $1/b$ between pulses, a whole q -element column of the codebook needs to be generated. Hence the required PRNG speed is $q \cdot b$ codebook entries per second, where each entry consists of multiple bits depending on the fine-grainedness of the implementation. Taking for example $q = 2^{10}$, $b = 2^{22}$ results in 2^{32} required entries per second, versus the $\approx 2^{37}$ bits per second that one core can generate. For higher baud rates and larger q many parallel PRNGs will be needed, e.g. implemented on FPGAs.

Note that the quality of the pseudorandom bits may not need to be high. Good error-correcting properties are perhaps achievable with PRNGs that do not pass randomness test suites, and which produce far more bits per clock cycle.

Another computational bottleneck is that Alice needs to evaluate the function F_Y^{inv} for every single codebook entry. Fortunately, all sub-scores can be computed in parallel. The process can be speeded up by first determining all the possible discrete values of $c_i - w_{\ell_i}$ and then storing all the possible values of $F_Y^{\text{inv}}(c_i - w_{\ell_i} \bmod 1)$ in a lookup table (LUT). The squaring operation can similarly be precomputed. This would result in a two-dimensional LUT of sub-score values indexed by discrete values for x_i and $c_i - w_{\ell_i} \bmod 1$. Computing the score S_ℓ then reduces to counting how often each entry in the LUT occurs in the $\sum_{i=1}^n$ summation. It may be possible to store the whole LUT in cache, which can be accessed much faster than general RAM. Similarly, the scores S_1, \dots, S_q can be kept in cache while ‘under construction’.

References

- [1] S.J. Johnson, V.A. Chandrasetty, and A.M. Lance. Repeat-Accumulate codes for reconciliation in Continuous Variable Quantum Key Distribution. In *2016 Australian Communications Theory Workshop (AusCTW)*, pages 18–23.
- [2] M. Milicevic, C. Feng, L.M. Zhang, and P.G. Gulak. Key reconciliation with Low-Density Parity-Check codes for long-distance quantum cryptography. 2017. <https://arxiv.org/pdf/1702.07740.pdf>.
- [3] X. Jiang, S. Yang, P. Huang, and G. Zeng. High speed reconciliation for CVQKD based on spatially coupled LDPC codes. *IEEE Photon. J.*, 10:1–10, 2018.
- [4] D. Guo, C. He, T. Guo, Z. Xue, Q. Feng, and J. Mu. Comprehensive high-speed reconciliation for continuous-variable quantum key distribution. *Quantum Information Processing*, 19, 2020. Article number 320.
- [5] K. Gümüş, T.A. Eriksson, M. Takeoka, M. Fujiwara, M. Sasaki, L. Schmalen, and A. Alvarado. A novel error correction protocol for continuous variable quantum key distribution. *Scientific Reports*, 11, 2021. article number 10465.
- [6] P. Jouguet and S. Kunz-Jacques. High performance error correction for quantum key distribution using polar codes. *Quantum Information & Computation*, 14(3-4):329–338, 2014.
- [7] M. Zhang, H. Hai, Y. Feng, and X.-Q. Jiang. Rate-adaptive reconciliation with polar coding for continuous-variable quantum key distribution. *Quantum Information Processing*, 20, 2021. Article number 318.
- [8] S. Yang, Z. Yan, H. Yang, Q. Lu, Z. Lu, L. Cheng, X. Miao, and Y. Li. Information reconciliation of continuous-variables quantum key distribution: principles, implementations and applications. *EPJ Quantum Technology*, 10, 2023. article number 40.

- [9] Ü.M. Maurer. Secret key agreement by public discussion from common information. *IEE Trans. on Information Theory*, pages 733–742, 1993.
- [10] M.J. Gander and Ü.M. Maurer. On the secret-key rate of binary random variables. In *ISIT'94*, page 351, 1994.
- [11] Jaromír Fiurášek and Nicolas J. Cerf. Gaussian postselection and virtual noiseless amplification in continuous-variable quantum key distribution. *Phys. Rev. A*, 86:060302, Dec 2012.
- [12] Miguel Navascués, Frédéric Grosshans, and Antonio Acín. Optimality of gaussian attacks in continuous-variable quantum cryptography. *Phys. Rev. Lett.*, 97:190502, Nov 2006.
- [13] A. Leverrier, R. Alléaume, J. Boutros, G. Zémor, and P. Grangier. Multidimensional reconciliation for a continuous-variable quantum key distribution. *Phys.Rev.A*, 77:042325, 2008.
- [14] G. Van Assche, J. Cardinal, and N.J. Cerf. Reconciliation of a quantum-distributed Gaussian key. *IEEE Transactions on Information Theory*, 50(2):394–400, 2004.
- [15] S.J Johnson, A.M Lance, L. Ong, M. Shirvanimoghaddam, T.C. Ralph, and T. Symul. On the problem of non-zero word error rates for fixed-rate error correction codes in continuous variable quantum key distribution. *New J. of Physics*, 19:023003, 2017.
- [16] S. Pirandola, R. Laurenza, C. Ottaviani, and L. Banchi. Fundamental limits of repeaterless quantum communications. *Nat.Comm.*, 8(15043), 2017.
- [17] Xiangyu Wang, Menghao Xu, Yin Zhao, Ziyang Chen, Song Yu, and Hong Guo. Non-gaussian reconciliation for continuous-variable quantum key distribution. *Phys. Rev. Appl.*, 19:054084, May 2023.
- [18] Florian Kanitschar and Christoph Pacher. Optimizing continuous-variable quantum key distribution with phase-shift keying modulation and postselection. *Phys. Rev. Appl.*, 18:034073, Sep 2022.
- [19] A. Leverrier. *Theoretical study of continuous-variable quantum key distribution*. Phd thesis, Télécom ParisTech, Nov 2009.
- [20] S. Yamano, T. Matsuura, Y. Kuramochi, T. Sasaki, and M. Koashi. General treatment of Gaussian trusted noise in continuous variable quantum key distribution, 2023. <https://arxiv.org/abs/2305.17684>.
- [21] A. Marie and R. Alléaume. Self-coherent phase reference sharing for continuous-variable quantum key distribution. *Phys.Rev.A*, 95:012316, 2017.
- [22] I. Devetak and A. Winter. Distillation of secret key and entanglement from quantum states. *Proc.R.Soc.A*, 461:207–235, 2005.
- [23] F. Laudenbach, C. Pacher, C.-H.F. Fung, A. Poppe, M. Peev, B. Schrenk, M. Hentschel, P. Walther, and H. Hübel. Continuous-Variable Quantum Key Distribution with Gaussian Modulation—The Theory of Practical Implementations. *Advanced Quantum Technologies*, 1(1):1870011, 2018.
- [24] Michael M. Wolf, Geza Giedke, and J. Ignacio Cirac. Extremality of gaussian quantum states. *Phys. Rev. Lett.*, 96:080502, Mar 2006.
- [25] Raúl García-Patrón and Nicolas J. Cerf. Unconditional optimality of gaussian attacks against continuous-variable quantum key distribution. *Phys. Rev. Lett.*, 97:190503, Nov 2006.
- [26] Matthias Heid and Norbert Lütkenhaus. Security of coherent-state quantum cryptography in the presence of gaussian noise. *Phys. Rev. A*, 76:022313, Aug 2007.
- [27] Anthony Leverrier. Security of continuous-variable quantum key distribution via a gaussian de finetti reduction. *Phys. Rev. Lett.*, 118:200501, May 2017.

- [28] R. Renner and J. I. Cirac. de finetti representation theorem for infinite-dimensional quantum systems and applications to quantum cryptography. *Phys. Rev. Lett.*, 102:110504, Mar 2009.
- [29] Anthony Leverrier. Composable security proof for continuous-variable quantum key distribution with coherent states. *Phys. Rev. Lett.*, 114:070501, Feb 2015.
- [30] K. Gümüř, J. dos Reis Frazão, A. Albores-Mejia, B. Škorić, G. Liga, Y. Can Gültekin, T. Bradley, A. Alvarado, and C. Okonkwo. Information reconciliation for continuous-variable Quantum Key Distribution beyond the Devetak-Winter bound using short blocklength error correction codes, 2024. <https://arxiv.org/abs/2409.13667>.
- [31] M. Tomamichel, C. Schaffner, A. Smith, and R. Renner. Leftover Hashing Against Quantum Side Information. *IEEE Transactions on Information Theory*, 57(8):5524–5535, 2011.
- [32] S. Vigna. Further scramblings of Marsaglia’s xorshift generators. *Journal of Computational and Applied Mathematics*, 315:175–181, 2017.
- [33] MWC256 algorithm. <https://prng.di.unimi.it/>.